AIP | Chaos
An Interdisciplinary Journal of Nonlinear Science
25TH ANNIVERSARY

Elimination of a spiral wave pinned at an obstacle by a train of plane waves: Effect of diffusion between obstacles and surrounding media

Masanobu Tanaka, Marcel Hörning, Hiroyuki Kitahata, and Kenichi Yoshikawa

Citation: Chaos **25**, 103127 (2015); doi: 10.1063/1.4934561
View online: http://dx.doi.org/10.1063/1.4934561
View Table of Contents: http://scitation.aip.org/content/aip/journal/chaos/25/10?ver=pdfcov
Published by the AIP Publishing

Elimination of a spiral wave pinned at an obstacle by a train of plane waves: Effect of diffusion between obstacles and surrounding media

Masanobu Tanaka,[1] Marcel Hörning,[2] Hiroyuki Kitahata,[3,a)] and Kenichi Yoshikawa[4]
[1]*Department of Physics, Graduate School of Science, Kyoto University, Kyoto 606-8502, Japan*
[2]*Institute for Integrated Cell-Material Sciences, Kyoto University, Kyoto 606-8501, Japan*
[3]*Department of Physics, Graduate School of Science, Chiba University, Chiba 263-8522, Japan*
[4]*Faculty of Life and Medical Sciences, Doshisha University, Kyotanabe, Kyoto 610-0394, Japan*

(Received 28 July 2015; accepted 12 October 2015; published online 27 October 2015)

In excitable media such as cardiac tissue and Belousov-Zhabotinsky reaction medium, spiral waves tend to anchor (pin) to local heterogeneities. In general, such pinned waves are difficult to eliminate and may progress to spatio-temporal chaos. Heterogeneities can be classified as either the absence or presence of diffusive interaction with the surrounding medium. In this study, we investigated the difference in the unpinning of spiral waves from obstacles with and without diffusive interaction, and found a profound difference. The pacing period required for unpinning at fixed obstacle size is larger in case of diffusive obstacles. Further, we deduced a generic theoretical framework that can predict the minimal unpinning period. Our results explain the difference in pacing periods between for the obstacles with and without diffusive interaction, and the difference is interpreted in terms of the local decrease of spiral wave velocity close to the obstacle boundary caused in the case of diffusive interaction. © *2015 AIP Publishing LLC*. [http://dx.doi.org/10.1063/1.4934561]

Spiral waves can be observed in diverse reaction-diffusion systems, such as the Belousov-Zhabotinsky (BZ) reaction medium, aggregation of starving slime mold amoeba, and cardiac tissue. It is known that propagation of a spiral wave in cardiac tissue is associated with life-threatening diseases, such as tachyarrhythmias and ventricular fibrillation. To eliminate such dangerous spiral waves, various methods are proposed: one of them is anti-tachycardia pacing (ATP). However, when there are heterogeneities in the media, such as non-excitable regions, a spiral wave may get pinned to them and thus is more difficult to be eliminated. Therefore, the investigation of unpinning of spiral waves from heterogeneities is important. In the present study, we discuss the mechanism of unpinning from heterogeneities, i.e., obstacles, by considering the diffusive interaction between the obstacle and the surrounding medium. The insights obtained in the present study regarding the effect of diffusive interaction on unpinning contribute to the future clinical improvement of anti-tachycardia pacing methods.

I. INTRODUCTION

Spiral waves are characteristic patterns that are generated in excitable media, and are found in a rich variety of systems, such as the BZ reaction, catalytic reactions on platinum surfaces, the aggregation of starving slime mold amoeba, and the action potential in cardiac tissue.[1–6] There are two basic types of waves in excitable media: target and spiral patterns. The former is generated by spatial heterogeneities or fluctuations in the local dynamics of the excitable medium, like a high-frequency source. In contrast, stable spiral waves are observed even in the absence of spatial heterogeneities or fluctuations, and if there are spatial heterogeneities or fluctuations, spiral waves are often trapped by them. Thus, over the past several decades, analytical and numerical studies have greatly advanced our understanding of the dynamics of spiral waves generated in homogeneous media.

Recently, there has been growing interest in spiral waves generated in inhomogeneous excitable media.[7] One example is the work by Steinbock and Müller, where the spiral core was controlled by the application of a laser spot in photo-sensitive BZ reaction for the first time.[8] Further studies on the unpinning of spiral waves have been investigated on the control and unpinning of spiral waves in the BZ reaction.[9,10] A more prominent system besides BZ reaction is cardiac tissue where spiral waves can be induced and pinned to local heterogeneities (obstacles) such as blood vessels and scar tissues. Spiral waves in the heart are believed to be precursors of life-threatening cardiac tachyarrhythmias, which often proceed to ventricular fibrillation and finally sudden death.[11,12] For this reason, methods for the removal of spiral waves are considered to be highly important for the medical treatment of cardiac arrhythmias. The suppression of spiral waves by high-frequency electrical stimulation, known as ATP, is one of the most successful methods developed so far.[13,14] Recently, it has been suggested that ATP can terminate spiral waves through the induced drift of the spiral tip to the boundary of cardiac tissue. It has been shown that the spiral starts to drift due to the influence of waves emitted by an external high-frequency source.[15] Free spiral waves can be easily eliminated when the frequency of electrical stimulation is just slightly higher than that of the spiral wave. However, when spiral waves are pinned to obstacles, it

a)Author to whom correspondence should be addressed. Electronic mail: kitahata@chiba-u.jp

becomes difficult to induce drift of the spiral tip and subsequently to cause termination. To induce drift of the spiral tip, the spiral wave must be first detached from the obstacle. This is only possible when the pacing source has a much higher frequency than that of the pinned spiral wave.[14,16]

In the present study, we classified obstacles, to which spiral waves are pinned, into two types based on the absence or presence of diffusive interaction with the surrounding medium, as hard and soft obstacles, respectively. Hard obstacles are "classical" non-excitable areas within the medium, and soft obstacles exhibit lower excitability than the surrounding medium and diffusive interaction.

To date, most studies on unpinning have focused on hard obstacles. With regard to hard obstacles, we have recently theoretically derived the dependency of the pacing period required for unpinning on the obstacle radius.[9,17] In contrast, although a few studies have investigated the unpinning pacing period of spiral waves pinned to soft obstacles by means of computer simulations,[18] the mechanism has not yet been clarified.

Here, we numerically investigated the mechanism of unpinning in the case of soft obstacles in comparison with hard obstacles, and theoretically discussed the differences focusing on the unpinning process. Additionally, we verified the unpinning process by experiments using the photosensitive BZ reaction.

II. NUMERICAL SIMULATION

To clarify differences in unpinning between hard and soft obstacles, we performed numerical simulations using the modified Oregonator model which is known to adequately describe the dynamics of the photosensitive BZ reaction,[19,20] with respect to the position $\mathbf{r}$ as

$$\begin{cases} \dfrac{\partial u}{\partial t} = \dfrac{1}{\epsilon}\left[u(1-u) - (fv + \phi(\mathbf{r}))\dfrac{u-q}{u+q}\right] + D\nabla^2 u, \\ \dfrac{\partial v}{\partial t} = u - v, \end{cases} \tag{1}$$

where $u(\mathbf{r}, t)$ and $v(\mathbf{r}, t)$ are the concentrations of the activator ($HBrO_2$) and the oxidized catalyst ($[Ru(bpy)_3]^{3+}$), respectively. We adopt Eq. (1) because the photosensitive BZ reaction is known to be an easily controllable excitable system; pinning to heterogeneities has also been reported in this experimental system.[9] The parameters ϵ, f, and q are positive values that determine the characteristics of the BZ reaction. In this study, we consider the following values, $\epsilon = 0.1$, $f = 2$, and $q = 2 \times 10^{-3}$, which are similar to those in our previous study.[9] D is the diffusion constant of the activator. For simplicity, the diffusion constant of the oxidized catalyst (v) is taken to be zero. In the present study, we choose a two-dimensional system to study the effect of diffusive interaction in a simple system. The calculation is performed in cylindrical coordinates. The computational domain is set to be a circle, whose radius is 15. The Neumann boundary condition is adopted for the outer boundary. The spatiotemporal resolution is $\Delta t = 2 \times 10^{-5}$, $\Delta r = 0.1$, and $\Delta\theta = \pi/200$. We used the Euler method, and the time step was taken so that the stability condition, $r > \sqrt{D\Delta t/2}/\Delta\theta \approx 0.2$, is satisfied.

$\phi(\mathbf{r})$ is a variable that is proportional to the light intensity, and can be described as

$$\phi(r,\theta) = \begin{cases} \phi_{\text{obs}} & \text{if } r \le R \\ \phi_{\text{med}} & \text{otherwise}, \end{cases} \tag{2}$$

where R is the obstacle radius.

In this numerical simulation, spiral waves are generated and pinned to the obstacles. For both hard and soft obstacles, we set $\phi_{\text{med}} = 0.01$ and $D = 1.0$ in the region surrounding the obstacle.

In the present study, we gave soft obstacles, which exhibit a certain degree of diffusive interaction, lower excitability than the surrounding medium. In the photosensitive BZ reaction, light illumination decreases the excitability[21] and the illuminated area exhibits diffusive interaction with the surrounding area in the aqueous chemical reaction. Thus, the region illuminated by high-intensity light is regarded as a soft obstacle. In the case of soft obstacles, in the present study we set $\phi_{\text{obs}} = 0.20$ and $D = 1.0$ at the periphery of the obstacle. These values prohibit wave propagation within the obstacle, but allow diffusion of the activator.

On the other hand, for hard obstacles, we set a Neumann boundary condition at the periphery of the obstacle. This condition prohibits diffusion of the activator at the boundary of the obstacle. Since such an obstacle has no diffusive interaction with its surrounding area, it is considered to be a hard obstacle.

To treat unpinning in a quantitative manner, we focus on the activator of the pinned spiral wave at the periphery of the obstacle. Under the application of a wave train, the activator of a pinned wave tends to be depressed at the periphery of the obstacle. If the pacing period is sufficiently small, the pinned wave unpins and shifts to a free spiral. As a control system, we investigated a free spiral wave in the region surrounding the obstacle. Under the condition that $D = 1.0$ and $\phi = 0.01$, a free spiral wave exhibits rigid rotation and the tip traces a circle with a radius of $R_{\text{free}} = 1.6$. The activator of the tip of the circle ($r \le R_{\text{free}}$) is less than 0.01. Thus, if the activator of a pinned wave becomes lower than 0.01 at the periphery of the obstacle, it is regarded to be unpinning since the pinned wave shifts to a free spiral. Furthermore, if the unpinned wave drifts to the system boundary and is eventually annihilated, it is regarded to have been eliminated.

We classify the behavior of pinned spiral waves whether they can be classified as unpinning or eliminated. We found that spiral waves on soft obstacles exhibit three different patterns of unpinning, as shown in Fig. 1, where the obstacle radius is fixed at $R = 3.0$.

Figure 1(a) shows an example of successful unpinning and elimination. Wave S_0, pinned to an obstacle, rotates counterclockwise ($t = 10$). At a pacing period of $T_p = 4.5$, wave 1 hits the obstacle, and separates into a wave rotating counterclockwise (1a) and a wave rotating clockwise (1b) ($t = 12$). Waves S_0 and 1b collide and merge, leaving only one rotating wave 1a, denoted S_1 hereafter ($t = 13$). The activator of wave S_1 is depressed at the periphery of the obstacle

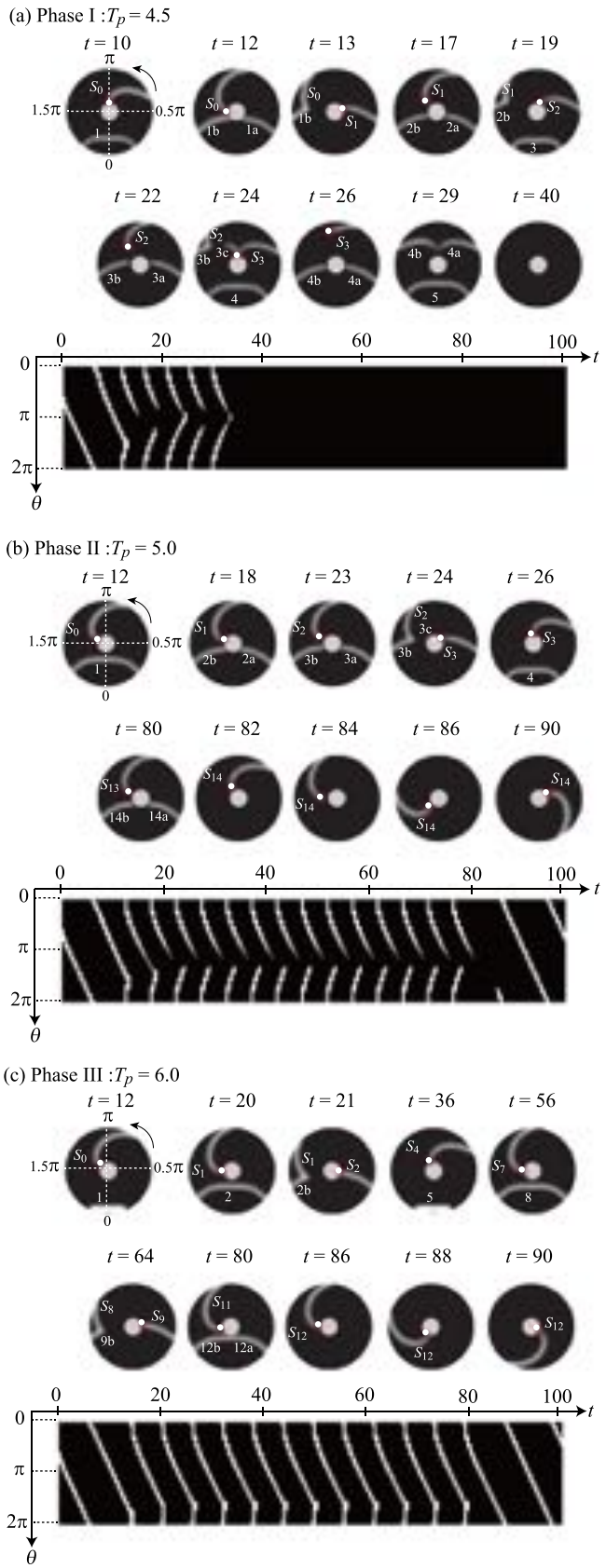

FIG. 1. Numerical examples of the effect of a wave train for three phases in case of soft obstacles. The size of the obstacle is fixed to be $R = 3.0$. The spiral tips are marked by white dots. The wave train is applied between $t = 0$ and $t = 29$ in (a) and between $t = 80$ in (b) and (c). (a) Successful unpinning and elimination with $T_p = 4.5$. (b) Successful unpinning but the failure of elimination with $T_p = 5.0$. (c) Unsuccessful unpinning with $T_p = 6.0$. The spatiotemporal diagrams show the changes with time in the activator concentration at the periphery of the obstacle.

and becomes lower than 0.01. Thus, wave S_1 unpins ($t = 17$). The unpinned wave S_1 and 2b collide and merge, leaving only one rotating wave S_2 in the same way as leaving S_1 ($t = 19$). Wave S_2 unpins and goes farther than S_1 from the obstacle ($t = 22$). A wave 3c is produced after collision of waves S_2 and 3b ($t = 24$). The wave 3c collides with S_3 and the tip of S_3 drifts away from the obstacle ($t = 26$). The tip collides with the outer boundary and is annihilated. Thus, a pinned spiral wave is eliminated from the system. After that, a pair of the counterclockwise (4a) and clockwise waves (4b) annihilate each other at $\theta = \pi$ ($t = 29$). During the application of the wave train, this process repeats. The wave train is stopped at $t = 29$, and no wave propagates ($t = 40$). Thus, the spiral tip detaches from the obstacle and is eliminated (phase I).

In contrast, Figure 1(b) shows an example of successful unpinning but a failure of elimination. At a pacing period of $T_p = 5.0$, the activator of wave S_1 is higher than 0.01 at the periphery of the obstacle. Thus, wave S_1 does not unpin ($t = 18$). The activator of wave S_2 is depressed at the periphery of the obstacle and becomes lower than 0.01. Thus, wave S_2 unpins ($t = 23$). Since the tip of S_2 does not get away as far from the obstacle as the above case of $T_p = 4.5$, a produced wave 3c is so small that it vanishes before it collides the following spiral wave S_3 ($t = 24$). Thus, the tip of S_3 does not drift away from the obstacle ($t = 26$), but only unpins in the same way as S_2. In a similar manner, the spiral wave $S_n (n = 4–13)$ unpins but does not drift away. After stopping the wave train at $t = 80$, the tip of S_{14} unpins from the obstacle once ($t = 82$), and gets close to it again ($t = 86$). The tip is finally repinning ($t = 90$). In other words, the spiral wave temporarily detaches (unpinning), but is not eliminated (phase II).

At a pacing period of $T_p = 6.0$, the spiral tip does not detach from the obstacle (phase III), as shown in Fig. 1(c). During the application of the wave train, the activator of wave $S_n (n = 1–12)$ is higher than 0.01 at the periphery of the obstacle. Thus, the pinned spiral wave does not unpin, and continues to annihilate with the clockwise-rotating wave at the periphery of the obstacle.

Thus, we can characterize three phases depending on the pacing period as follows: Phase I, successfully unpins and eliminates the spiral; phase II, temporary unpinning; and phase III, no apparent effect on the spiral wave. We note that the initial location of the spiral wave around the object does not concern whether the unpinning succeeded or not. Details are shown in Fig. S1 in the supplementary material.[22]

Here, with a hard obstacle, it is noted that phase II is not observed. Therefore, the unpinned wave inevitably drifts and is eventually annihilated at the boundary of the medium. Examples can be found in Fig. S2 in the supplementary material.[22]

However, this dependency is rather different from the previous result by Pumir *et al.*[16] We anticipate that this is caused by the difference in an obstacle radius R. Pumir *et al.* studied the unpinning phenomena in the case of $R < R_{\text{free}}$. On the other hand, in the present study, we study on the case that $R > R_{\text{free}}$.

Based on the results of a numerical study on parameter-dependence, we deduce the phase diagrams for both cases. Figures 2(a) and 2(b) show the phase diagrams for soft and hard obstacles, respectively. These show the dependency of the pacing period T_p required for unpinning or elimination at an obstacle radius R. Figure 2(b) corresponds to the same dependence as shown previously.[9] In both cases, the pacing period T_p required for unpinning and elimination decreases with an increase in the obstacle radius. It has been confirmed that the thresholds of the phases do not change with prolonged pacing.

In the case of soft obstacles, the boundary between phases II and III determines the maximum pacing period T_{unp} required for unpinning. The results confirm that T_{unp} is essentially independent of the light intensity ϕ_{obs} for $0.02 \leq \phi_{\mathrm{obs}} \leq 0.20$ (see Fig. S4 in the supplementary material[22]). Thus, regardless of the light intensity ϕ_{obs}, T_{unp} for soft obstacles is larger than that for hard obstacles. Thus, apparently, spiral waves that are pinned to soft obstacles are easier to unpin than those that are pinned to hard obstacles.

III. THEORY

We start the theoretical argument regarding unpinning phenomena by considering the shape and velocity of a spiral wave that is pinned to an obstacle. The shape of a pinned spiral wave was studied by Tyson and Keener.[23] In their framework, the curvature effect of the pinned spiral wave is taken into account by adopting the following linear Eikonal equation:

$$V = V_0 + D\kappa, \tag{3}$$

where V is the wave velocity affected by the curvature, V_0 is the velocity of a plane wave, and κ is the curvature of the wave front. If the wave front curves away from its direction of propagation, κ is a negative. From the geometrical relationship, the velocity and curvature can be derived as

$$\begin{aligned} V &= \frac{\omega r}{\sqrt{1+\psi^2}}, \\ \kappa &= \frac{d\psi/dr}{\left(1+\psi^2\right)^{\frac{3}{2}}} + \frac{1}{r}\frac{\psi}{\left(1+\psi^2\right)^{\frac{1}{2}}}, \end{aligned} \tag{4}$$

where ω is the angular velocity of the pinned wave, ψ is defined as $\psi \equiv r d\theta_s/dr$; $\theta_s(r)$ is the angle of the tangential vector from a certain direction, depending on the distance from the origin, r. Thus, $\theta_s(r)$ can be regarded as the representation of the wave shape, because it uniquely determines the shape of the wave at a given time. By substituting Eq. (4) into Eq. (3), we obtain the following basic equation for the function $\psi(r)$:

$$-r\frac{d\psi}{dr} = \frac{rV_0}{D}\left(1+\psi^2\right)^{\frac{3}{2}} - \frac{\omega r^2}{D}\left(1+\psi^2\right) + \psi\left(1+\psi^2\right), \tag{5}$$

which can be solved analytically depending on the kind of obstacle.

A. Velocity of spiral waves pinned to hard obstacles (revisited)

First, we consider the case of a hard obstacle based on the above-mentioned framework by Keener and Tyson.[23] In this case, the velocity of a plane wave V_0 corresponds to the dispersion relation (restitution relation) $c_0(T_p)$, which denotes the wave front velocity of a wave train that is paced at a constant period T_p. It can be obtained by numerical calculation in a one-dimensional system based on the following equations:

$$\begin{cases} \dfrac{\partial u}{\partial t} = \dfrac{1}{\epsilon}\left[u(1-u) - (fv + I_0)\dfrac{u-q}{u+q}\right] + D\dfrac{\partial^2 u}{\partial x^2}, \\ \dfrac{\partial v}{\partial t} = u - v, \end{cases} \tag{6}$$

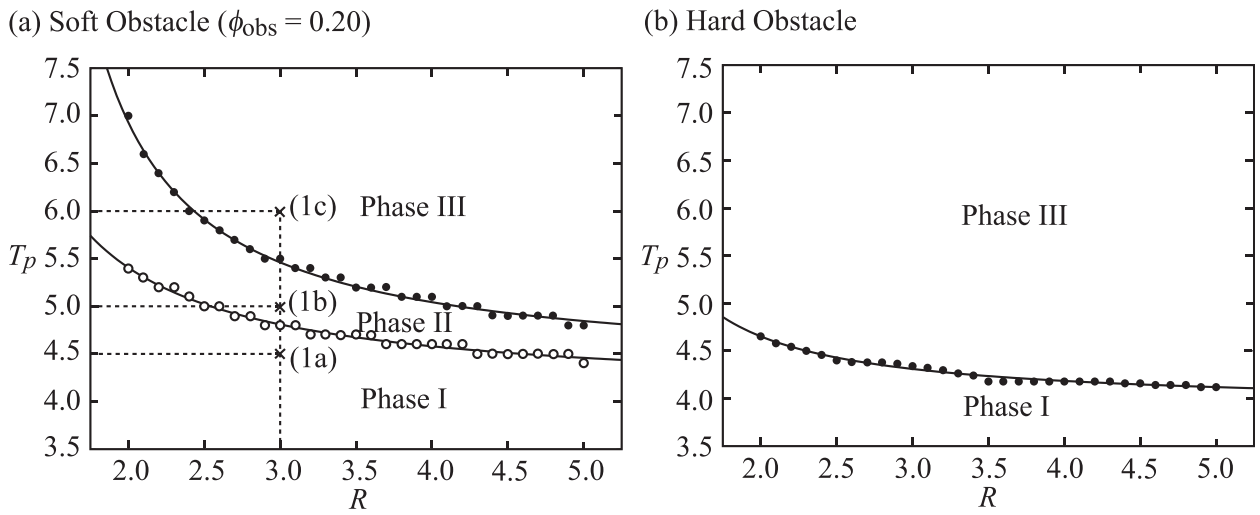

FIG. 2. Numerical results regarding the phases of unpinning and elimination, showing the wave train period as a function of the obstacle radius. Black and white points correspond to the pacing period T_p required for unpinning and elimination, respectively. (a)The phase diagram for soft obstacles. The three marked points correspond to the examples shown in Fig. 1. (b)The phase diagram in the case of hard obstacles. The solid lines are guides showing the thresholds.

where I_0 and D are set at $I_0 = \phi_{\text{med}} = 0.01$ and $D = 1.0$, respectively.

A no-flux condition is applied to the boundary of the hard obstacle, since the obstacle does not diffusively interact with the surrounding medium. Thus, the pinned spiral wave propagates perpendicularly to the periphery of the hard obstacle ($(d\theta_s/dr)|_{r=R} = 0$), as shown in Fig. 3(a), [23] which means that $\psi_{\text{hard}}\ (r=R) = 0$. Far from the obstacle, it is assumed that $\psi_{\text{hard}}\ (r) \sim \omega r/c_0$ for large r, since the pinned wave can be regarded as the plane wave with wave number ω/c_0. In the case of a hard obstacle, we set the following approximate solution of Eq. (5), which satisfies the above-mentioned two conditions:

$$\psi_{\text{hard}}(\bar{r}) = \alpha\frac{\bar{r}}{R} + \frac{\beta\bar{r}}{R+\gamma\bar{r}}, \tag{7}$$

with

$$\begin{cases} \alpha = -\dfrac{1+4\bar{c}-\sqrt{1+8\bar{c}}}{4(1+\bar{c})}, \\ \beta = \dfrac{1-\sqrt{1+8\bar{c}}}{4}, \\ \gamma = \dfrac{1+\sqrt{1+8\bar{c}}}{16}, \end{cases}$$

where $\bar{c} \equiv c_0 R/D$, $\bar{r} \equiv r - R$, and c_0 is obtained by the dispersion relation of the wave train (restitution relation). Furthermore, by using the Eikonal equation, Eq. (3), we derive the velocity of the pinned spiral V_{hard} as

$$V_{\text{hard}}(\bar{r}; R, c_0(T_p)) = c_0 + D\left\{\frac{d\psi_{\text{hard}}/dr}{\left(1+\psi_{\text{hard}}^2\right)^{\frac{3}{2}}} + \frac{1}{R+\bar{r}}\frac{\psi_{\text{hard}}}{\left(1+\psi_{\text{hard}}^2\right)^{\frac{1}{2}}}\right\}, \tag{8}$$

where ψ_{hard} is given by Eq. (7). $V_{\text{hard}}(\bar{r})$ represents the velocity of the pinned spiral at a distance $\bar{r}$ from the periphery of the hard obstacle.

B. Description of the effect of diffusive interaction from soft obstacles

In the case of a soft obstacle, we have to consider the diffusive interaction between the pinned spiral and the obstacle, as well as the curvature effect. The following two points are the most significant in the case of a soft obstacle.

First, the pinned spiral wave does not propagate perpendicularly to the periphery of a soft obstacle ($\psi_{\text{soft}}\ (r=R) \neq 0$), as shown schematically in Figs. 3(b) and 3(c), since the soft obstacle exhibits diffusive interaction. Second, diffusive interaction leads to a gradient of the activator, as shown in Figs. 3(b) and 3(d). In the proximity of the obstacle, this gradient leads to diffusion of the activator from the wave front to the soft obstacle. Thus, we have to modify the above-mentioned framework for a hard obstacle.

(i) The pinned spiral wave does not propagate perpendicularly to the periphery of the obstacle, but the shape of the pinned spiral wave is deformed ($(d\theta_s/dr)|_{r=R} > 0$), as shown schematically in Fig. 3(c). To describe ψ_{soft} similarly to Eq. (7), we define the effective radius of the soft obstacle $R_{\text{eff}}\ (= R + \Delta R)$ as

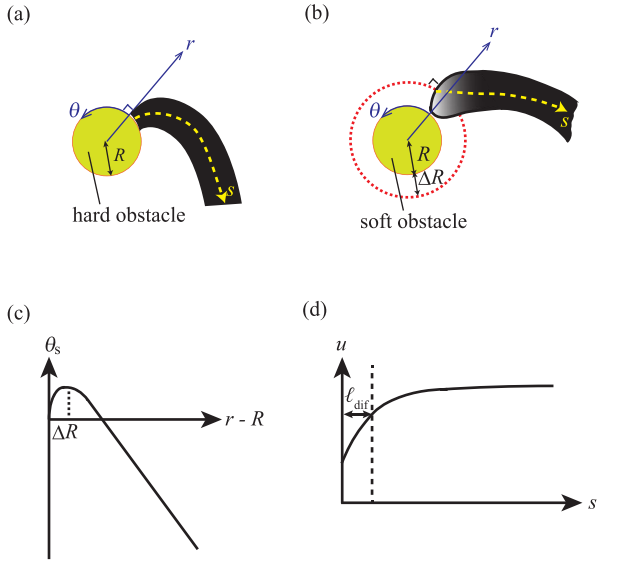

FIG. 3. Schematic representation of the two types of pinned spiral waves. (a) and (b) Illustrations of spiral waves pinned to a hard obstacle and a soft obstacle, respectively. (c) The shape of the wave front $\theta_s(r)$ on a soft obstacle. (d) The distribution of u in a spiral wave pinned to a soft obstacle. ℓ_{dif} is the effective range of the diffusive interaction, shown in Eq. (11). Here, s represents the arc length along the wave.

$$\left.\frac{d\theta_s}{dr}\right|_{r=R_{\text{eff}}} = 0. \tag{9}$$

(ii) Since the activator of the spiral wave diffuses to the obstacle due to diffusive interaction, we change Eq. (1) with consideration for this effect as follows:

$$\begin{cases} \dfrac{\partial u}{\partial t} = \dfrac{1}{\epsilon}\left[u(1-u) - (fv+I_0)\dfrac{u-q}{u+q}\right] - F(r,u) + D\nabla^2 u, \\ \dfrac{\partial v}{\partial t} = u - v, \end{cases} \tag{10}$$

where $F(r, u)$ represents the effect due to diffusion of the activator, which decreases to zero with an increase in the distance from the soft obstacle. Considering this property of $F(r, u)$, we assume

$$F(r,u) = \delta\ \exp\left(-\frac{r-R_{\text{eff}}}{\ell_{\text{dif}}}\right)u, \tag{11}$$

where δ is a positive number that indicates the degree of the effect of the diffusion of the activator and ℓ_{dif} is the effective length of diffusive interaction. Through this assumption, it becomes possible for us to discuss the unpinning process analytically by only considering the wave propagation outside of the obstacle, since the effect of the obstacle is simply represented by the function $F(r, u)$.

C. Velocity of plane waves affected by diffusive interaction

To determine the velocity of a spiral wave that is pinned to a soft obstacle, first we derive the velocity of a plane wave

V_0 affected by diffusive interaction, neglecting the effect of curvature. Here, the effect of diffusive interaction is represented by the addition of the term $F(r, u)$ considering Eq. (10). Thus, we add $F(r, u)$ to Eq. (6) as follows:

$$\begin{cases} \dfrac{\partial u}{\partial t} = \dfrac{1}{\epsilon}\left[u(1-u) - (fv + I_0)\dfrac{u-q}{u+q}\right] - F(r,u) + D\dfrac{\partial^2 u}{\partial x^2}, \\ \dfrac{\partial v}{\partial t} = u - v, \end{cases} \tag{12}$$

where we adopt Eq. (11) as the diffusive effect $F(r, u)$. V_0 is determined using Eq. (12).

The effect of $F(r, u)$ on the velocity V_0 of a single plane wave can be written as Eq. (S10), whose derivation is shown in the supplementary material.[22] We assume that the effect of $F(r, u)$ (Eq. (S10)) is also applied to the dispersion relation c_0 in the same manner, that is,

$$V_0 = c_0\left(1 - \frac{1}{2}\epsilon\delta \exp\left(-\frac{\bar{r}'}{\ell_{\mathrm{dif}}}\right)\right). \tag{13}$$

Next, we derive the velocity of a spiral wave pinned to a soft obstacle while considering the effect of curvature. Here, the curvature of the pinned spiral wave at the periphery of the soft obstacle $\kappa(r = R_{\mathrm{eff}})$ is set as κ_0. Since the pinned spiral wave propagates perpendicularly to the periphery of the obstacle with an effective radius of R_{eff}, the velocity of a pinned spiral wave V $(r = R_{\mathrm{eff}})$ corresponds to ωR_{eff}. Thus, by using the Eikonal equation, Eq. (3), we can derive the condition that $\omega R_{\mathrm{eff}} = c_0(1 - \epsilon\delta/2) + D\kappa_0$.

Since Eq. (13) has to satisfy this condition, the velocity of a plane wave affected by diffusive interaction V_0 can be derived as

$$V_0(\bar{r}') = c_0\left\{1 - \left(1 - \frac{\omega R_{\mathrm{eff}} - D\kappa_0}{c_0}\right)\exp\left(-\frac{\bar{r}'}{\ell_{\mathrm{dif}}}\right)\right\}. \tag{14}$$

Note that the velocity of the plane wave V_0 depends on the distance $\bar{r}'$ from the periphery of the soft obstacle. In other words, as a consequence of diffusive interaction, V_0 in the proximity of the soft obstacle has a smaller value than the dispersion relation c_0.

D. Velocity of spiral waves pinned to soft obstacles

Finally, we consider the shape of a spiral wave that is pinned to a soft obstacle with an effective radius of R_{eff} by Eq. (5). The solution of Eq. (5) can be approximated for the two specific ranges: For $r \simeq R_{\mathrm{eff}}$,

$$\begin{aligned} \psi_{\mathrm{soft}}(\bar{r}') = {} & \bar{\kappa}'\left(\frac{\bar{r}'}{R_{\mathrm{eff}}}\right) \\ & + \left\{\frac{1}{2}\left(\bar{\omega}' - \bar{\kappa}' - (\bar{\omega}' - \bar{c}' - \bar{\kappa}')\frac{R_{\mathrm{eff}}}{\ell_{\mathrm{dif}}}\right)\right\}\left(\frac{\bar{r}'}{R_{\mathrm{eff}}}\right)^2 \\ & + \mathcal{O}(\bar{r}'^3), \end{aligned} \tag{15}$$

and for $r \to \infty$,

$$\psi_{\mathrm{soft}}(\bar{r}') = -\frac{\bar{\omega}'}{\bar{c}'}\left(\frac{\bar{r}'}{R_{\mathrm{eff}}}\right) - \frac{\bar{\omega}'}{\bar{c}'}\left(1 + \frac{1}{\bar{c}'}\right) + \mathcal{O}\left(\frac{1}{\bar{r}'}\right), \tag{16}$$

where R_{eff} is the effective radius which is defined in Eq. (9), $\bar{r}' \equiv r - R_{\mathrm{eff}}$, $\bar{c}' \equiv c_0 R_{\mathrm{eff}}/D$, $\bar{\omega}' \equiv \omega R_{\mathrm{eff}}^2/D$, and $\bar{\kappa}' \equiv \kappa_0 R_{\mathrm{eff}}$.

The general solution of Eq. (5) is obtained, which reduces to Eq. (15) in the limit of $\bar{r}' \to 0$ and Eq. (16) in the limit of $\bar{r}' \to \infty$, as follows:

$$\psi_{\mathrm{soft}}(\bar{r}') = \alpha'\frac{\bar{r}'}{R_{\mathrm{eff}}} + \frac{\beta'\bar{r}'}{R_{\mathrm{eff}} + \gamma'\bar{r}'}, \tag{17}$$

with

$$\begin{cases} \alpha' = -\dfrac{\bar{\omega}'}{\bar{c}'}, \\ \beta' = \bar{\kappa}' + \dfrac{\bar{\omega}'}{\bar{c}'}, \\ \gamma' = -\left(1 + \bar{\kappa}'\dfrac{\bar{c}'}{\bar{\omega}'}\right)\left(\dfrac{\bar{c}'}{\bar{c}'+1}\right). \end{cases}$$

The effective length of the diffusive interaction ℓ_{dif} in Eq. (14) is defined as follows:

$$\frac{1}{\ell_{\mathrm{dif}}} = \frac{1}{R_{\mathrm{eff}}}\frac{1}{\bar{c}' - \bar{\omega}' + \bar{\kappa}'}\left\{\bar{\omega}' - \bar{\kappa}' - 2\frac{(\bar{\omega}' + \bar{\kappa}'\bar{c}')^2}{\bar{\omega}'(\bar{c}'+1)}\right\}. \tag{18}$$

Finally, using the Eikonal equation, Eq. (3), we obtain the velocity of the pinned spiral V_{soft} as

$$\begin{aligned} V_{\mathrm{soft}}\left(\bar{r}'; R_{\mathrm{eff}}, c_0(T_p)\right) = {} & V_0(\bar{r}') + D\left\{\frac{d\psi_{\mathrm{soft}}/dr}{\left(1 + \psi_{\mathrm{soft}}^2\right)^{\frac{3}{2}}}\right. \\ & \left. + \frac{1}{R_{\mathrm{eff}} + \bar{r}'}\frac{\psi_{\mathrm{soft}}}{\left(1 + \psi_{\mathrm{soft}}^2\right)^{\frac{1}{2}}}\right\}, \end{aligned} \tag{19}$$

where $V_0(\bar{r}')$ and ψ_{soft} are given by Eqs. (14) and (17), respectively. $V_{\mathrm{soft}}(\bar{r}')$ represents the velocity of the pinned spiral at a distance $\bar{r}'$ from the periphery of the soft obstacle with an effective obstacle radius R_{eff}.

IV. DISCUSSION

We propose a common theory of unpinning in the both cases for a pinned spiral wave with a velocity $V_{\mathrm{hard}}(\bar{r})$ or $V_{\mathrm{soft}}(\bar{r}')$. When unpinning occurs, a pinned spiral wave does not propagate within the proximity of the obstacle, and a portion of the pinned spiral wave disappears. To explain the unpinning phenomena, we consider the disappearance of a plane wave. When plane waves are initiated at a pacing period of T_p, there is a critical period T_p^*, below which the wave train cannot be initiated. This means that if the wave velocity of a plane wave V_0 is lower than the critical velocity $c_0^* = c_0(T_p^*)$, the plane wave fails to propagate and disappears.

Going back to the unpinning phenomena, we define the width of the disappearing portion of a spiral wave as L, which is comparable to the width of the wave. The velocities at a distance of L from the periphery of hard and soft obstacles, V_{hard} (L) and V_{soft} (L), are shown in Fig. 4. To

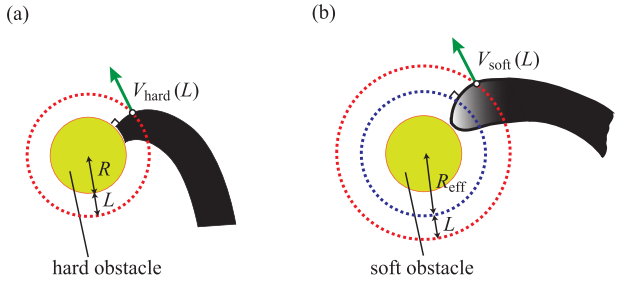

FIG. 4. Illustrative drawing of the velocities of pinned spiral waves: $V_{\rm hard}(L)$ and $V_{\rm soft}(L)$. L is the width of the disappearing portion of a spiral wave in the process of unpinning, which is comparable to the width of the wave. (a) $V_{\rm hard}(L)$ is the velocity at a distance L from the periphery of a hard obstacle with radius R. (b) $V_{\rm soft}(L)$ is the velocity at a distance L from the periphery of a soft obstacle with an effective radius $R_{\rm eff}$.

explain the unpinning phenomena, we have to compare $V_{\rm hard}(L)$ and $V_{\rm soft}(L)$ with the critical velocity c_0^*. When $V_{\rm hard}(L)$ and $V_{\rm soft}(L)$ are below the critical velocity c_0^*, a portion of a spiral wave disappears within the proximity of the obstacle and unpinning occurs. Thus, $V_{\rm hard}(L) = c_0^*$ and $V_{\rm soft}(L) = c_0^*$ determine the pacing period required for unpinning $T_{\rm unp}$ for hard and soft obstacles, respectively.

In our theoretical model, it is assumed that the width of the disappearing portion L depends exclusively on the excitability of the medium. Thus, L is independent of both the boundary condition at the periphery of the obstacle and the obstacle radius R, and L is a common value for both hard and soft obstacles. This means that the difference in the pacing period required for unpinning $T_{\rm unp}$ between the two cases is due to the presence or absence of the diffusive interaction, which is included in Eq. (19) for $V_{\rm soft}(\bar{r}')$. To verify that the proposed theory of unpinning is valid for our numerical results, we calculate the critical period T_p^* and the critical velocity c_0^* using Eq. (6). In the area surrounding the obstacle under our numerical simulation, T_p^* and c_0^* are calculated to be $T_p^* = 3.50$ and $c_0^* = 2.81$, respectively.

First, for a hard obstacle, the width of the disappearing portion of a spiral wave L can be calculated, which satisfies $V_{\rm hard}(L; R, c_0(T_{\rm unp})) = c_0^*$, at the unpinning boundary in Fig. 2(b). As a result, $L = 0.63 \pm 0.08$ in the range of $2.0 \le r_0 \le 5.0$. On the other hand, the width of the wave is estimated to be approximately 1 from snapshots in Fig. 1. The average value of L is comparable to the width of a wave ($\simeq 1$).

To clarify the validity of the proposed theory in the case of a hard obstacle, we analytically deduce the pacing period required for unpinning $T_{\rm unp}$ from $V_{\rm hard}(L; R, c_0(T_{\rm unp})) = c_0^*$. Since it is assumed in the proposed theory that L is independent of the obstacle radius R, the value of L is fixed to be 0.63 in the calculation. A relationship between R and $T_{\rm unp}$ is obtained, which satisfies $V_{\rm hard}(L; R, c_0(T_{\rm unp})) = c_0^*$. The result is shown as a dashed curve in Fig. 5. This dashed curve is consistent with the numerical results in a case of hard obstacle. Thus, the proposed theory of unpinning is valid in the case of hard obstacle.

Furthermore, we can also verify that the proposed theory of unpinning is valid in the case of a soft obstacle. Since it is assumed in the proposed theory that the width of the

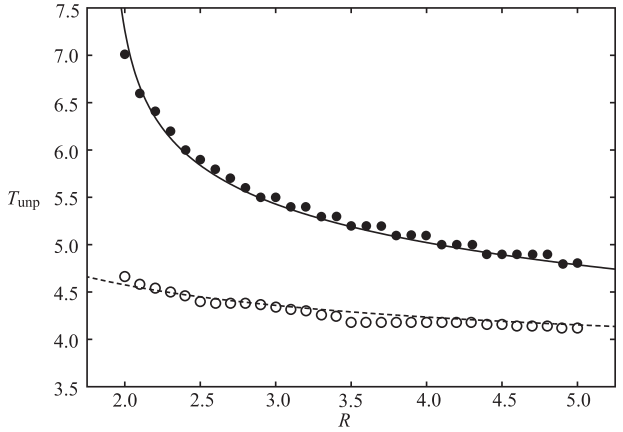

FIG. 5. Comparison of the numerical and theoretical results. The closed (open) circles are numerical results, which represent the relationship between the obstacle radius R and the pacing period required for unpinning $T_{\rm unp}$ in the case of a soft (hard) obstacle. The numerical results are the same as those shown in Figs. 2(a) and 2(b). The solid and dashed curves represent the respective theoretical results, which are deduced from $V_{\rm soft}(L; R + \Delta R, c_0(T_{\rm unp})) = c_0^*$ and $V_{\rm hard}(L; R, c_0(T_{\rm unp})) = c_0^*$.

disappearing portion L is a common value in both cases, the value of L is also fixed to be 0.63 in the case of a soft obstacle. We analytically deduce the relationship between R and $T_{\rm unp}$ from $V_{\rm soft}(L; R_{\rm eff}, c_0(T_{\rm unp})) = V_{\rm soft}(L; R + \Delta R, c_0(T_{\rm unp})) = c_0^*$ using the following values: $\Delta R = -1.79/R + 1.83$, $\bar{\kappa}' = 1.98/R - 2.63$, $\ell_{\rm dif} = -1.63/R + 2.22$, which are the approximated values of ΔR, A_1 and $\ell_{\rm dif}$ at the unpinning boundary in Fig. 2(a). The details are shown in the supplementary material.[22] The results are shown as a solid curve in Fig. 5. This solid curve is consistent with the numerical results in the case of a soft obstacle. Thus, we conclude that the proposed common theory of unpinning is also valid in the case of a soft obstacle.

V. EXPERIMENTAL VERIFICATION OF THE UNPINNING OF SPIRAL WAVES FROM HARD AND SOFT OBSTACLES

To confirm the validity of our numerical results and theory, experiments were performed on a membrane filter (Advantec, A100A025A), which was soaked in a solution for the photosensitive BZ reaction with ruthenium (Ru) catalysts.[24,25] Diffusion of BZ solution is restricted on the membrane filter and this experimental system can be regarded as a quasi-two-dimensional system, which is appropriate to confirm the results by numerical simulation in a two-dimensional system. The concentrations in the BZ solution are $[NaBrO_3] = 0.6\,M$, $[H_2SO_4] = 0.3\,M$, $[CH_2(COOH)_2] = 0.2\,M$, $[NaBr] = 0.05\,M$, and $[Ru(bpy)_3Cl_2] = 1.7\,mM$. On this filter, spiral waves were generated, which were pinned to both types of obstacles. In our previous study, we created a hard obstacle by putting a small droplet of silicone oil on the filter (Fig. 6(a)).[9] Since the region in which the oil was soaked was protected from the BZ solution, there was no reaction solution in this region. Though there should be diffusion of a small amount of neutral chemical species like bromine in the oil, this effect is considered to be negligibly small and thus we regard the oil-soaked region as a hard obstacle. Furthermore, as a soft

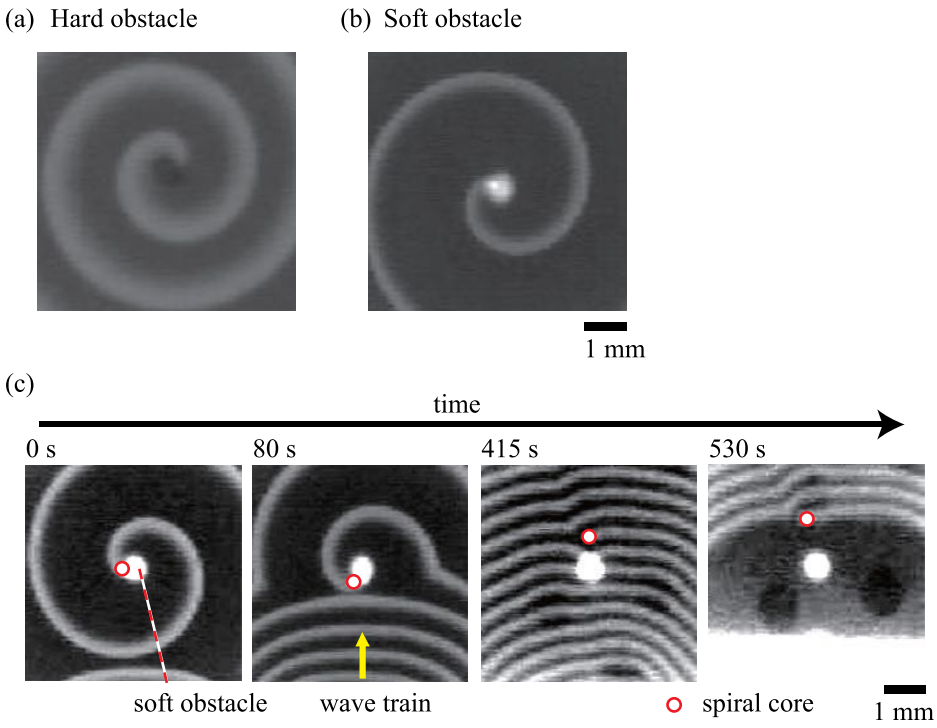

FIG. 6. Experimental observation of high-frequency unpinning in the excitable BZ reaction. (a) and (b) Pinned spirals on hard and soft obstacles, respectively. (c) An example of the unpinning process of a spiral anchored on a soft obstacle. The wave train approaching from the bottom led to unpinning at $t \approx 400$ s. The unpinned spiral wave was forced to drift upward together with subsequent traveling waves. The waves of the train were suppressed by strong light illumination of 60 klx at $t \approx 470$ s to verify detachment of the spiral, i.e., accomplishment of the unpinning.

obstacle, we produced a high-intensity light spot on the filter using a liquid-crystal projector (Fig. 6(b)). The obstacle radius was set to approximately 0.5 mm ($R \simeq 0.5$ mm). The light intensities in the high-intensity light spot and in the surrounding area were 60 klx and 0.5 klx, respectively. The light intensity on the membrane filter was measured with a light-intensity meter (AS ONE, LX-100). Figures 6(a) and 6(b) show experimental examples of spiral waves pinned to a hard and a soft obstacle, respectively. The wavelength around the hard obstacle was smaller than that around the soft obstacle, which is caused by the difference in the spiral period and the interaction with the obstacle. The same tendency was observed in numerical simulations as seen in Fig. S6 in the supplementary material.[22] Additionally, small differences in the experimental conditions such as temperature and light intensity are found to cause an enhanced difference.

To deliver wave trains to the pinned wave around the soft obstacle, we produced a high-frequency source of excitation by applying a micro-droplet of sulfuric acid to the outer boundary of the filter. Figure 6(c) shows the snapshots of the experimental observation of the unpinning process around the soft obstacle. The generated wave train approached the pinned wave and entrained the whole filter. The wave-train period on the obstacle was 13 s ($T_p = 13$ s). At $t \approx 400$ s, the pinned wave detached from the obstacle, and the subsequent waves pushed the detached wave away from the obstacle.

Thus, our experimental observations have provided the validity of the essential difference between soft and hard obstacles on unpinning. However, we faced difficulties that the reproducibility of the experimental trends was not so satisfactory, because small changes in the initial chemical concentrations dominated the resulting BZ dynamics. Future experiments on some of excitable media to verify our theoretical and numerical expectations are awaited.

VI. CONCLUSION

In the present paper, we investigated the unpinning of the spiral wave from soft obstacles under diffusive interaction by expanding the theoretical framework from the model of hard obstacles. We calculated the critical unpinning frequency by utilizing the dispersion relation of plane waves. Further, we performed numerical simulations using the modified Oregonator model to investigate the similarities and differences in the unpinning process of spiral waves from hard and soft obstacles. The simulations revealed that the pacing period T_{unp} required for unpinning at a fixed obstacle radius in the case of a soft obstacle is larger than that in the case of a hard obstacle.

The mechanism of unpinning in both cases is discussed by taking into account the diffusive interaction between the obstacle and its surrounding medium. We focused on the velocity $V(L)$ of the wave front in the proximity of the obstacle. A general theory of unpinning is proposed, in which unpinning occurs when the velocity $V(L)$ is below a critical wave velocity c_0^*.

We analytically deduced the relationships between the size of the obstacle R and the required period T_{unp} required for unpinning. The results showed that our proposed theory can be applied to both cases, since the unpinning relationships deduced from our theory are consistent with the numerical results, as shown in Fig. 5. Our results indicate that the difference in the pacing period T_{unp} required for unpinning between the two cases is interpreted in terms of a decrease in velocity caused by diffusive interaction.

The insights obtained in this study regarding the effect of diffusive interaction on unpinning are expected to contribute to the future development of anti-tachycardia pacing. Although our proposed theory is consistent with the numerical results, further studies are necessary on the effects of cell

orientation, the electroelastic properties of cardiac tissue, obstacles with complex shapes (vessel-like, scar-like) and three-dimensional effects, which may help to improve current medical applications.[26,27]

ACKNOWLEDGMENTS

This work was partly supported by a Grants-in-Aid for Scientific Research on Innovative Areas "Fluctuation & Structure" (No. 25103012) to K.Y. and (No. 25103008) to H.K. from the Ministry of Education, Culture, Sports, Science, and Technology of Japan.

[1]R. Kapral and K. Showalter, *Chemical Waves and Patterns* (Kluwer Academic, Dordrecht, 1995).
[2]A. T. Winfree, Science **175**, 634 (1972).
[3]S. Jakubith, H. Rotermund, W. Engel, A. V. Oertzen, and G. Ertl, Phys. Rev. Lett. **65**, 3013 (1990).
[4]E. Pálsson and E. C. Cox, Proc. Natl. Acad. Sci. U. S. A. **93**, 1151 (1996).
[5]J. M. Davidenko, A. V. Pertsov, R. Salomonsz, W. Baxter, and J. Jalife, Nature **355**, 349 (1992).
[6]F. X. Witkowski, L. J. Leon, P. A. Penkoske, W. R. Giles, M. L. Spano, W. L. Ditto, and A. T. Winfree, Nature **392**, 78 (1998).
[7]C. Cherubini, S. Filippi, and A. Gizzi, Phys. Rev. E **85**, 031915 (2012).
[8]O. Steinbock and S. C. Müller, Physica A **188**, 61 (1992).
[9]M. Tanaka, A. Isomura, M. Hörning, H. Kitahata, K. Agladze, and K. Yoshikawa, Chaos **19**, 043114 (2009).
[10]Z. Z. Jiménez, Z. Zhang, and O. Steinbock, Phys. Rev. E **88**, 052918 (2013).
[11]R. A. Gray, J. Jalife, A. V. Panfilov, W. T. Baxter, C. Cabo, J. M. Davidenko, A. M. Pertsov, A. V. Panfilov, P. Hogeweg, and A. T. Winfree, Science **270**, 1222 (1995).
[12]A. T. Winfree, Chaos **8**, 1 (1998).
[13]K. Agladze, M. W. Kay, V. Krinsky, and N. Sarvazyan, Am. J. Physiol. Heart Circ. Physiol. **293**, 503 (2007).
[14]A. Isomura, M. Hörning, K. Agladze, and K. Yoshikawa, Phys. Rev. E **78**, 066216 (2008).
[15]V. I. Krinsky and K. I. Agladze, Physica D **8**, 50 (1983).
[16]A. Pumir, S. Sinha, S. Sridhar, M. Argentina, M. Hörning, S. Filippi, and C. Cherubini, Phys. Rev. E **81**, 010901 (2010).
[17]M. Hörning, A. Isomura, Z. Jia, E. Entcheva, and K. Yoshikawa, Phys. Rev. E **81**, 056202 (2010).
[18]Y.-Q. Fu, H. Zhang, Z. Cao, B. Zheng, and G. Hu, Phys. Rev. E **72**, 046206 (2005).
[19]J. J. Tyson and P. C. Fife, J. Phys. Chem. **73**, 2224 (1980).
[20]H. J. Krug, L. Pohlmann, and L. Kuhnert, J. Phys. Chem. **94**, 4862 (1990).
[21]S. Kádár, T. Amemiya, and K. Showalter, J. Phys. Chem. **101**, 8200 (1997).
[22]See supplementary material at http://dx.doi.org/10.1063/1.4934561 for the detailed derivation and the results of the numerical calculations.
[23]J. J. Tyson and J. P. Keener, Physica D **32**, 327 (1988).
[24]L. Kuhnert, Nature **319**, 393 (1986).
[25]L. Kuhnert, Naturwissenschaften **73**, 96 (1986).
[26]M. Hörning, Phys. Rev. E **86**, 031912 (2012).
[27]P. Kuklik, P. Sanders, L. Szumowski, and J. J. Zebrowski, J. Biol. Phys. **39**, 67 (2012).